Journal of Petroleum Science and Engineering 175 (2019) 184–189

Contents lists available at ScienceDirect

Journal of Petroleum Science and Engineering

journal homepage: www.elsevier.com/locate/petrol

Milled basalt fiber reinforced Portland slurries for oil well applications

Luanna Carla Matias Paiva[a,*], Irantécio Mendonça Ferreira[a], Antonio Eduardo Martinelli[b], Julio Cezar de Oliveira Freitas[c], Ulisses Targino Bezerra[d]

[a] Federal University of Rio Grande do Norte (UFRN), Cement Laboratory, Natal, RN, 59072-970, Brazil
[b] Federal University of Rio Grande do Norte (UFRN), Dept. Materials Engineering, Natal, RN, 59072-970, Brazil
[c] Federal University of Rio Grande do Norte (UFRN), Chemical Institute, Natal, RN, 59072-970, Brazil
[d] Federal Institute of Paraíba (IFPB), Civil Construction, Academic Unit 1, João Pessoa, PB, 58015-430, Brazil

ARTICLE INFO

Keywords:
Basalt fiber
Oil well cement
Portland cement
Silica flour

ABSTRACT

The dispersion of short fibers to oil well Portland slurries may improve the compressive strength and fracture energy of the hardened cementing material. A study was carried out to investigate the effect of the addition of ball-milled basalt fibers (5% BWOC) to Portland slurries. Samples were prepared with and without silica flour (40% BWOC) in the composition and cured for 7 days under different Bottom Hole Static Temperatures (BHST): 80 °C (176 °F) and 300 °C (572 °F). The mechanical properties and the microstructure of the hardened pastes were evaluated by compressive strength tests, X-ray diffraction and scanning electron microscopy. The results showed that milling basalt fibers was a cost efficient method to adjust the length of the basalt wool fibers assuring slurry mixing and, therefore, adequate pumpability. The combined addition of silica flour and basalt fibers improved the fracture energy of samples cured at 80 °C, therefore below the strength retrogression temperature. Curing at 300 °C resulted in significant fiber consumption by pozzolanic reactions that could not be prevented by the addition of silica flour. Therefore, ball-milled basalt fibers can be a cost-efficient and environmental-friendly solution to improve the mechanical properties of oil well cement slurries used below the retrogression temperature.

1. Introduction

Long-term production of oil and gas rely on cementing materials capable of withstanding crack growth and propagation, therefore ensuring the integrity of the cement sheath (Anjos et al., 2013; Costa et al., 2017; Han et al., 2011; Ichim and Teodoriu, 2017; Silva et al., 2018; Mangadlao et al., 2015; Soares et al., 2015; Souza et al., 2018). To that end, the addition of short fibers potentially increases the fracture energy of Portland-based cement materials (Bentur and Mindess, 2007). Different fibers have been used to reinforce Portland cement slurries, including polypropylene, polyvinyl (Qiu et al., 2017), polyacetal (Yang et al., 2017), steel (Beglarigale, 2017), carbon (Chen et al., 2018), cellulose (Cheng et al., 2018) and glass fibers (Khorami et al., 2017). Each type of fiber depicts advantages and limitations regarding density, geometrical aspects (length, diameter and aspect ratio), bonding to the cement matrix, and evidently cost and benefit. Studies have reported the potential use of basalt fibers (Anandamurthy et al., 2017; Fiore et al., 2015; Jalasutram et al., 2017; Jiang et al., 2014; Katkhuda and Shatarat, 2017; Ren et al., 2016; Vejmelková et al., 2018). On the downside, Berndt and Philippacopoulos (2002) have also studied the addition of different fibers, including basalt fibers, to class-G geothermal well cements containing 40% silica flour. They observed that the addition of 0.5% and 1.0% basalt fibers, 6 mm and 15 mm long, negatively affected the uniformity of the dispersion and the tensile strength of the hardened material.

Ball milled basalt fibers can meet most technical requirements at relatively low production costs. Care must be taken regarding the combination of high service temperatures and alkaline environments, since it can affect the integrity of basalt fibers due to its silica-rich composition. Cheng et al. (2018) studied oil well cement slurries reinforced with cellulose fibers that are also susceptible to alkaline environment. The addition of 15% silica fume improved both the mechanical strength and durability of the slurries. Khorami et al. (2017) tested Portland cement reinforced by silica-rich glass fibers with the addition of nanosilica. The pozzolanic reaction along with the filler action of nanosilica resulted in strong bonding at the fiber-cement interfacial zone. The durability of the matrix was also improved by the decrease in porosity and permeability.

Basalt fibers have also been used to reinforce concrete. Kabay (2014) observed that as the content of basalt fibers increased, the

* Corresponding author.
E-mail address: luannacm_paiva@yahoo.com.br (L.C.M. Paiva).

https://doi.org/10.1016/j.petrol.2018.11.068
Received 25 October 2018; Received in revised form 23 November 2018; Accepted 26 November 2018
Available online 14 December 2018
0920-4105/

Table 1
Composition of cement slurries (mass in g).

Sample	Cement	Fibers (5%)	Silica (40%)	Water	w/c ratio
BF0	765.67	0.00	0.00	355.91	0.46
BF5	734.48	36.72	0.00	350.38	0.48
BF0S40	560.84	0.00	224.34	336.40	0.60
BF5S40	543.92	27.20	217.57	332.89	0.61

strength of concrete not only increased, but also larger deflections before failure and higher fracture energy values were achieved. Dias and Thaumaturgo (2005) reported that the fracture toughness of concrete reinforced with basalt fibers exceeded that of conventional unreinforced samples.

The objective of the present study was to assess the service parameter limits for the use of milled basalt fibers to strengthen oil well Portland cement slurries. Portland-basalt fiber mixes were hardened under two different Bottom Hole Static Temperature (BHST), *i.e.* 80 °C (176 °F) and 300 °C (572 °F). The former accounts for high temperature and geothermal wells, and the latter for wells subjected to steam injection for enhanced oil recovery. The effect of adding silica flour (40% BWOC) and ball-milled basalt fibers (5% BWOC) on the mechanical properties of Portland cement slurry was studied. The microstructure of the hardened materials was also characterized by X-ray diffraction and scanning electron microscopy.

2. Materials and methods

The samples used in the scope of this study were prepared using Class A Special Portland cement (Votorantim S.A., Brazil), silica flour (Halliburton, Ltd., Brazil) containing approximately 99% SiO_2 (Shahab et al., 2015; Li et al., 2015) and basalt fiber (Larocha, Ltd., Brazil) purchased in the form of stone wool flakes. Water from the city supplier was also employed. The wool flakes were ball milled using alumina balls as grinding media. Each milling batch consisted of 30 g of flakes and 168 g of alumina balls, milled for 10 min. The cement pastes were formulated to depict density of 1.87 g/cm^3 (15.6 ppg). A summary of all compositions tested is listed in Table 1.

A Chandler 80-60 mixer was used to prepare the samples. Portland cement, silica flour and basalt fibers were previously and manually mixed and then added to water, as the mixer rotated at 4000 ± 200 rpm. The addition took place during 15 s. The speed was then increased to 12000 ± 500 rpm during 35 s, and the mixer was then turned off. The mixing protocol was established by the American Petroleum Institute (API, 2013) to reproduce the mixing energy reached by field mixers.

After mixing, the slurries were poured into metallic molds (50.8 mm edge) and soaked in a thermostatic bath at 80 °C for 7 days, which is representative of high temperature wells (HT). The procedure for curing at 300 °C consisted of 4 days in a thermostatic bath at 80 °C, followed by a thermal cycle of 3 days in a model Chandler 1910 curing chamber at 300 °C under 2000 psi. After curing, uniaxial compression tests were performed using three samples of each composition and for each curing temperature using a Shimadzu AG-I 100 kN Universal Mechanical Testing Machine. The software used to control the machine was the Trapezium 2. The fracture energy values were then calculated from the area under the load-displacement curves after maximum stress.

Crushed samples were selected for SEM and XRD analyses.

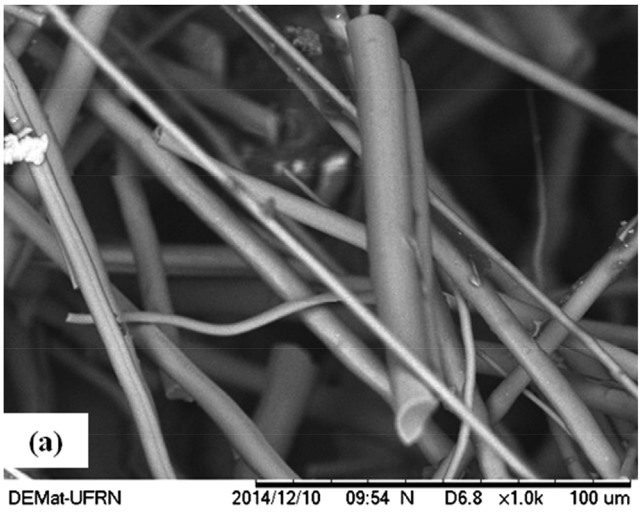

Fig. 1. SEM images of (a) pre-milled and (b) milled basalt fibers.

Micrographs were obtained using a HITACHI TM3000 SEM using backscattered electrons. Sample preparation consisted in depositing a small sample fragment onto a carbon adhesive tape attached to the sample holder. The diffractograms were obtained by a Bruker D8 Advance Eco set-up using CuKα radiation source set to 25 kV and 40 mA. Data were collected in the 2θ range from 5° to 80°. Each sample was crushed and pulverized using mortar and pestle. The software programs used in the phase identification were the EVA and TOPAS from Bruker.

3. Results and discussion

The chemical composition and morphology of the milled fibers can be seen in Table 2 and Fig. 1, respectively. The basalt fibers used in this study were received as long entangled filaments with chemical composition consisting of more than 50 wt% SiO_2, in addition to CaO, Fe_2O_3, and Na_2O as major constituents. A preliminary study was carried out to establish the minimum milling time of basalt wool flakes to

Table 2
Chemical composition of milled basalt fibers.

Composition	SiO_2	CaO	Fe_2O_3	Na_2O	Al_2O_3	MnO	MgO	SrO	K_2O	SO_3	Cr_2O_3
% wt	53.0	13.9	12.4	11.1	3.8	1.6	1.5	1.2	0.8	0.7	0.2

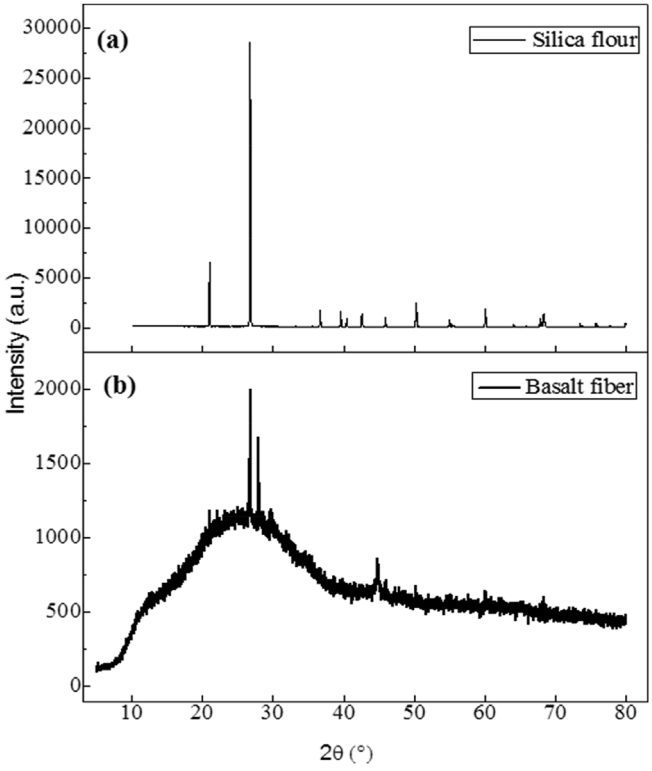

Fig. 2. XRD analysis: (a) silica flour and (b) basalt fiber.

assure proper rheology. Adding long fibers affects mixing, and therefore pumpability. Chena and Liub (2005) reported that fibers adsorb a considerable amount of cement slurry to wrap around, which increases the viscosity of the mixture. Milling not only reduced the length of basalt fibers, but also increased the roughness of the fiber surface, as can been in Fig. 1 (b). The latter can have a beneficial effect on the mechanical adhesion of the fiber to the cement matrix. Iorio et al. (2018) reported that certain treatments performed on the surface of commercial basalt fibers may be responsible for greater adhesion of fiber-matrix interfaces and durability of concrete based composite materials.

The XRD patterns of silica flour and milled fibers can be seen in Fig. 2. Whereas silica flour shows crystalline structure, basalt fibers are essentially amorphous and therefore reactive. The interaction between the fibers and Portland cement hydration products, especially calcium hydroxide (CH), can be increased under high temperature. To overcome this problem, the addition of silica flour (40% BWOC) can reduce the calcium hydroxide contents by means of the pozzolanic reaction to form C-S-H gel. The filler effect attributed to the fine particles also reduces the permeability of the hardened slurry.

The compressive strength and fracture energy of all compositions tested herein are shown in Fig. 3. The strength of the samples cured at 80 °C (Fig. 3a) increased with the addition of 5% basalt fibers, from ~23 MPa (BF0) to ~33 MPa (BF5). An increase in fracture energy from ~35 J (BF0S40) to 47 J (BF5S40) was also noticed from the combination of 5% basalt fibers with 40% silica flour. Such behavior can be related to the filler effect provided by silica flour at temperatures below 110 °C (Costa et al., 2017). The pozzolanic reaction between silica flour and calcium hydroxide in the pore solution of cement slurry is extremely slow at 80 °C (Ge et al., 2018). In addition, the increase in fracture energy in the fiber-reinforced cement slurry may be related to appropriate interfacial bonding, resulting from fiber milling. The effect of adding 40% silica flour to prevent the strength retrogression noticed in samples BF0 and BF5 is evident from samples cured at 300 °C (Fig. 3b) (Nelson and Guillot, 2006). The silica flour as well as the

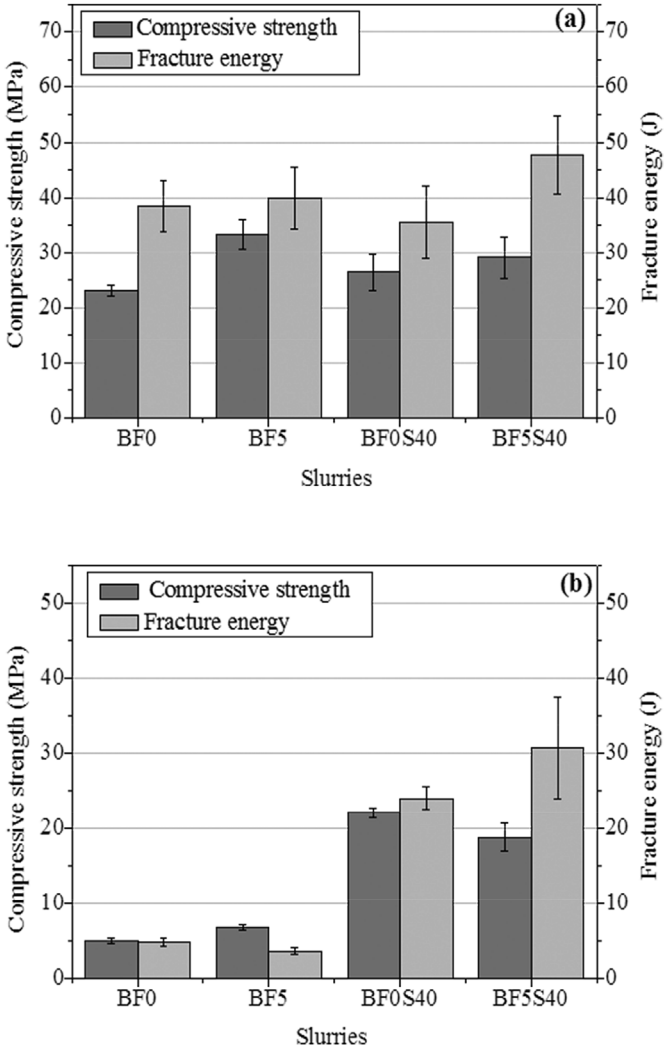

Fig. 3. Mechanical strength and fracture energy of samples cured at (a) 80 °C and (b) 300 °C.

basalt fibers were involved in the pozzolanic reactions, as sources of silica. The addition of basalt fibers showed little contribution to strength or fracture energy at 300 °C, contrary to what was observed in the samples cured at 80 °C. The silica flour acted as a source of silica in the pozzolanic reactions to form C-S-H gel, and no longer as filler in the microstructure of the cement matrix. The behavior observed for samples BF0S40 and BF5S40 suggests the formation of stable xonotlite phases, responsible for the mechanical strength at high temperature, as later confirmed by XRD analysis.

SEM images of samples cured at 80 °C and 300 °C can be seen in Fig. 4. The chemical interactions between the basalt fiber and the cement slurry (Sim et al., 2005), specifically between SiO_2 and calcium hydroxide (CH), are illustrated in Fig. 4 (a). The reactions involving basalt fiber (BF) and the cement slurry during the hydration process can be expressed as:

$$C_3S + H_2O \rightarrow \text{C-S-H gel} + CH \quad (1)$$

$$C_2S + H_2O \rightarrow \text{C-S-H gel} + CH \quad (2)$$

$$BF + CH + H_2O \rightarrow \text{C-S-H gel} \quad (3)$$

The reactions represented by equations (1) and (2) account for the hydration of C_3S and C_2S to form CH (Nelson and Guillot, 2006; Taylor, 1990). Reaction (3) shows the chemical interaction between BF and CH, which takes place as Si-O-Si bonds of the fiber which are broken by

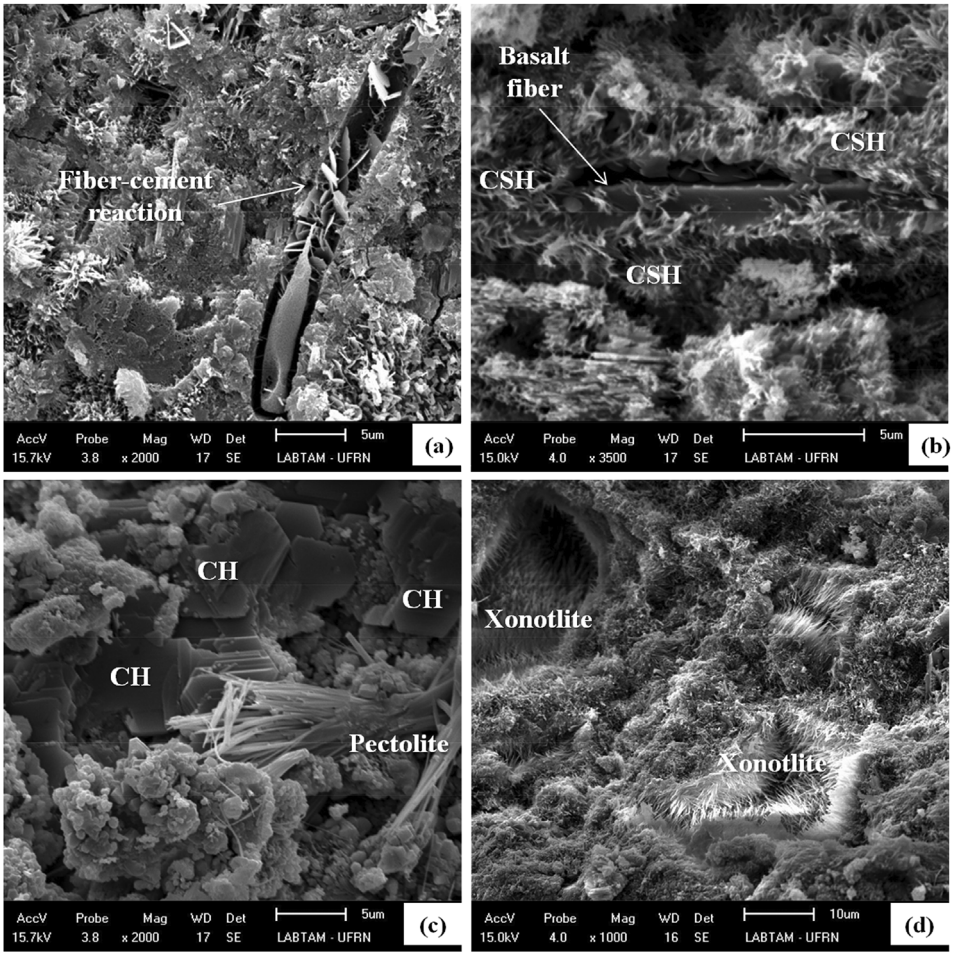

Fig. 4. SEM analysis of samples cured at 80 °C: (a) BF5 and (b) BF5S40; and 300 °C: (c) BF5and (d) BF5S40.

OH^- ions of the calcium hydroxide in solution (Bentur and Mindess, 2007).

Basalt fibers confined by amorphous C-S-H gel are illustrated in Fig. 4 (b) (Qiao et al., 2008). Milling may have contributed to better fiber-cement bonding. Moreover, the addition of silica flour could have acted towards reducing the porosity of the matrix by filling pores, which also increase the bonding between the fiber and the cement matrix. The combination of both effects improves the efficiency of fiber reinforcement, increasing the fracture energy of the cement.

The microstructure of BF5 sample cured at 300 °C is shown in Fig. 4 (c). The sample contained 5% BF and no silica flour. The fibers were likely consumed by the presence of CH (Hollis et al., 2006). In addition, well-developed broom-like pectolite formed, as can be seen in the microstructure (Nocun-Wczelik, 1999). Pectolite ($NaCa_2HSiO_3O_9$) is a sodium-containing calcium silicate phase that can be found in equilibrium with xonotlite, truscotite, foshagite and tobermorite.

The microstructure of BF5S40 sample, which contained 5% BF and 40% silica flour is shown in Fig. 4 (d). Due to the high curing temperature (300 °C), pozzolanic reactions involving both sources of silica (basalt fibers and silica flour) resulted in the formation of stable xonotlite [$Ca_6Si_6O_{17}(OH)_2$] (Ge et al., 2018).

The crystallographic characterization of the samples cured at 80 °C and 300 °C can be seen in Fig. 5 and Fig. 6, respectively. The main phases present after curing at 80 °C (Fig. 5) are ettringite, Portlandite (CH) and C-S-H gel. C-S-H gel was identified as a phase with low crystallinity (Richardson, 2008; Yanagisawa et al., 2006). Fig. 5 (a) and (b) show the presence of intense Portlandite peaks, similar to BF0 and BF5 samples, in addition to ettringite and C-S-H gel. Fig. 5 (c) and (d) show the presence of crystalline SiO_2 peaks corresponding to silica flour, in addition to ettringite, Portlandite and C-S-H gel. A small decrease in the intensity of Portlandite ($2\theta = \sim 18°$ and $\sim 34°$) and silica peaks ($2\theta = \sim 28°$) was noted for BF0S40 and BF5S40 samples. The addition of silica flour combined with basalt fibers improved the pozzolanic reactions for the formation of C-S-H gel. Therefore, the mechanical properties of the cement slurry might improve as a result of the proper bond between the hydrated products and the basalt fibers.

Fig. 6 (a) and (b) revealed the presence of Portlandite in samples BF0 and BF5. Differently from the behavior observed after curing at 80 °C, the addition of basalt fibers in the BF5 sample contributed to the pozzolanic reactions at 300 °C. Strength retrogression took place in the absence of silica flour above 110 °C. The presence of calcium chondrodite [$Ca_5(SiO_4)_2(OH)_2$] or reinhardbraunsite, responsible for most of the strength loss was also noticed (Anjos et al., 2013; Costa et al., 2017). The results corroborate the mechanical behavior observed in Fig. 3 (b). Fig. 6 (c) and (d) show more stable phases, such as xonotlite, which is formed above 150 °C by the conversion of tobermorite when the C/S ratio is close to 1.0 (Taylor, 1990). The basalt fibers along with silica flour contributed to the pozzolanic reactions. Contrary to what was observed from samples cured at 80 °C, xonotlite was observed instead of Portlandite.

4. Conclusions

The effect of adding ball-milled basalt fibers to oil well Portland cement slurries was investigated. The curing temperature as well as the presence of silica flour determined the microstructure, and therefore the mechanical properties of the hardened slurries. Curing at 80 °C revealed a material with high fracture energy by the combined addition of

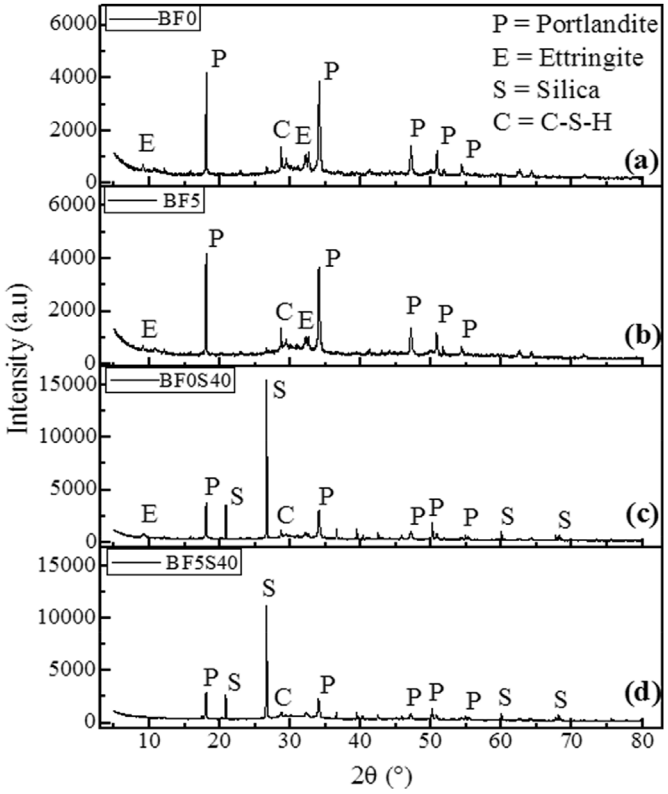

Fig. 5. XRD analysis of samples cured at 80 °C: (a) BF0, (b) BF5, (c) BF0S40 and (d) BF5S40.

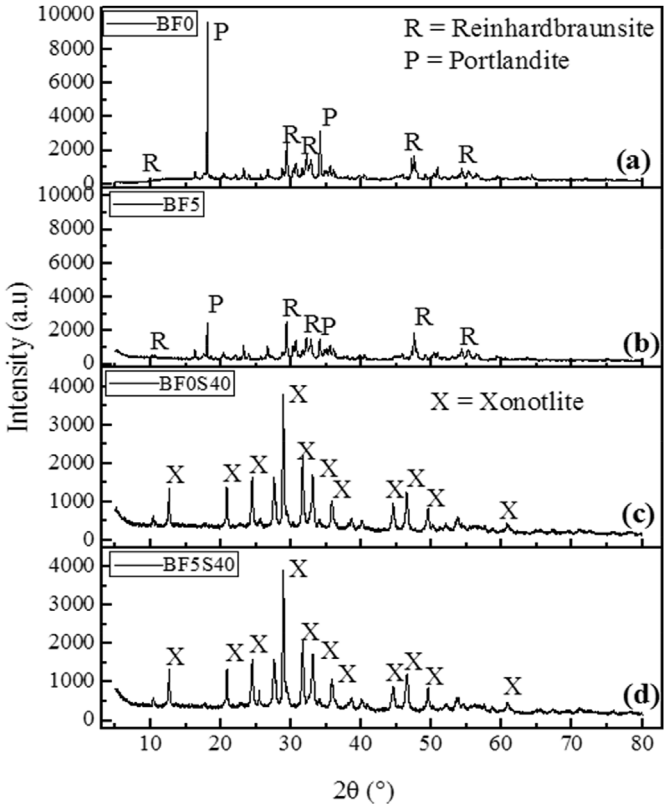

Fig. 6. XRD analysis of samples cured at 300 °C: (a) BF0, (b) BF5, (c) BF0S40 and (d) BF5S40.

silica flour (40% BWOC) and milled basalt fibers (5% BWOC), which resulted in an increase in fracture energy from ~35 J to 47 J. Curing at 300 °C resulted in strength retrogression of samples free from silica flour, regardless of the presence of basalt fibers. In addition, the basalt fibers were consumed by high temperature reactions due to their high contents of silica. Nevertheless, a slight increase in fracture energy was noticed due to the composition of the cement matrix. Therefore, the use of ball-milled basalt fibers is a cost-efficient and environmental solution to improve the fracture energy of oil well cement slurries used below the retrogression temperature.

Acknowledgements

The authors would like to thank Larocha Ltd. for the fibers supply, the Laboratory for Refining and Environmental Technology (LABTAM), Department of Materials Engineering (DEMAT/UFRN) and Cement Laboratory (LABCIM) for the availability of resources for the development of the study. This study was partly financed by the Coordenação de Aperfeiçoamento de Pessoal de Nível Superior - Brasil (CAPES) - Finance Code 001.

Appendix A. Supplementary data

Supplementary data to this article can be found online at https://doi.org/10.1016/j.petrol.2018.11.068.

References

Anandamurthy, A., Guna, V., Ilangovan, M., Reddy, N., 2017. A review of fibrous reinforcements of concrete. J. Reinforc. Plast. Compos. 36, 519–552.
Anjos, M.A.S., Martinelli, A.E., Melo, D.M.A., Renovato, T., Souza, P.D.P., Freitas, J.C., 2013. Hydration of oil well cement containing sugarcane biomass waste as a function of curing temperature and pressure. J. Petrol. Sci. Eng. 109, 291–297.
API, 2013. API Recommended Practice 10B-2-recommended Practice for Testing Well Cements, second ed. American Petroleum Institute, Washington.
Beglarigale, A., 2017. Electrochemical corrosion monitoring of steel fiber embedded in cement based composites. Cement Concr. Compos. 83, 427–446.
Bentur, A., Mindess, S., 2007. Fibre Reinforced Cementitious Composites, second ed. Taylor & Francis, London.
Berndt, M.L., Philippacopoulos, A., 2002. Incorporation of fibres in geothermal well cements. Geothermics 31, 643–656.
Chen, Z., Zhou, X., Wang, X., Guo, P., 2018. Mechanical behavior of multilayer GO carbon-fiber cement composites. Constr. Build. Mater. 159, 205–212.
Chena, B., Liub, J., 2005. Contribution of hybrid fibers on the properties of the high-strength lightweight concrete having good workability. Cement Concr. Res. 35, 913–917.
Cheng, X.W., Khorami, M., Shi, Y., Liu, K.Q., Guo, X.Y., Austin, S., Saidani, M., 2018. A new approach to improve mechanical properties and durability of low-density oil well cement composite reinforced by cellulose fibres in microstructural scale. Constr. Build. Mater. 177, 499–510.
Costa, B.L.S., Souza, G.G., Freitas, J.C.O., Araujo, R.G.S., Santos, P.H.S., 2017. Silica content influence on cement compressive strength in wells subjected to steam injection. J. Petrol. Sci. Eng. 158, 626–633.
Dias, D.P., Thaumaturgo, C., 2005. Fracture toughtness of geopolymeric concretes reinforced with basalt fibers. Cement Concr. Res. 27, 49–54.
Fiore, V., Scalici, T., Di Bella, G., Valenza, A., 2015. A review on basalt fiber and its composites. Compos. B Eng. 74, 74–94.
Ge, Z., Yao, X., Wang, X., Zhang, W., Yang, T., 2018. Thermal performance and microstructure of oil well cement paste containing subsphaeroidal konite flour in HTHP conditions. Constr. Build. Mater. 172, 787–794.
Han, B., Yu, X., Ou, J., 2011. Multifunctional and smart carbon nanotube reinforced cement-based materials. In: Gopalakrishnan, K., Birgisson, B., Taylor, P., Attoh-Okine, N. (Eds.), Nanotechnology in Civil Infrastructure. Springer, Berlin Heidelberg, pp. 1–47.
Hollis, N.W., Stephen, D.L., Stu, P.E., 2006. Petrographic Methods of Examining Hardened Concrete: a Petrographic Manual. Virginia, United States.
Ichim, A., Teodoriu, H.C., 2017. Investigations on the surface well cement integrityinduced by thermal cycles considering an improved overall transfer coefficient. J. Petrol. Sci. Eng. 154, 479–487.
Iorio, M.L., Santarelli, G., González-Gaitano, J., González-Benito, 2018. Surface modification and characterization of basalt fibers as potential reinforcement of concretes. Appl. Surf. Sci. 427, 1248–1256.
Jalasutram, S., Sahoo, D.R., Matsagar, V., 2017. Experimental investigation of the mechanical properties of basalt fiber-reinforced concrete. Struct. Concr. 36, 519–552.
Jiang, C., Fan, K., Wu, F., Chen, D., 2014. Experimental study on the mechanical properties and microstructure of chopped basalt fibre reinforced concrete. Mater. Des. 58, 187–193.

Kabay, N., 2014. Abrasion resistance and fracture energy of concretes with basalt fibre. Constr. Build. Mater. 50, 95–101.
Katkhuda, H., Shatarat, N., 2017. Improving the mechanical properties of recycled concrete aggregate using chopped basalt fibers and acid treatment. Constr. Build. Mater. 140, 328–335.
Khorami, M., Ganjian, E., Mortazavi, A., Saidani, M., Olubanwo, A., Gand, A., 2017. Utilisation of waste cardboard and Nano silica fume in the production of fibre cement board reinforced by glass fibres. Constr. Build. Mater. 152, 746–755.
Li, Z., Venkata, H.K., Rangaraju, P.R., 2015. Influence of silica flour–silica fume combination on the properties of high performance cementitious mixtures at ambient temperature curing. Constr. Build. Mater. 100, 225–233.
Mangadlao, J.D., Cao, P., Advincula, R.C., 2015. Smart cements and cement additives for oil and gas operations. J. Petrol. Sci. Eng. 129, 63–76.
Nelson, E.B., Guillot, D., 2006. In: Schlumberger, Sugar (Ed.), Well Cementing, Second. Land, Texas.
Nocun-Wczelik, W., 1999. Effect of Na and Al on the phases composition and morphology of autoclaved calcium silicate hydrates. Cement Concr. Compos. 29, 1759–1767.
Qiao, X.C., Tyrer, M., Poon, C.S., Cheeseman, C.R., 2008. Novel cementitious materials produced from incinerator bottom ash. Resour. Conserv. Recycl. 52, 496–510.
Qiu, J., Lim, X.N., Yang, E., 2017. Fatigue-induced in-situ strength deterioration of micro-polyvinyl alcohol (PVA) fiber in cement matrix. Cement Concr. Compos. 82, 128–136.
Ren, W., Xu, J., Su, H., 2016. Dynamic compressive behavior of basalt fiber reinforced concrete after exposure to elevated temperatures. Fire Mater. 40, 738–755.
Richardson, I.G., 2008. The calcium silicate hydrates. Cement Concr. Res. 38, 137–158.
Shahab, S., Moradi, T., Nikolaev, N.I., Naseri, Y., 2015. Developing High Resistant Cement Systems for High-pressure, High Temperature Applications. SPE Russian Petroleum Technology Conference, Moscow, Russia.
Silva, I.B., Martinelli, A.E., Souza, W.R.M., Freitas, J.C.O., Rodrigues, M.A.F., 2018. Dilatometric behavior and crystallographic characterization of Portland-polyurethane composites for oilwell high-temperature cementing applications. J. Petrol. Sci. Eng. 169, 553–559.
Sim, J., Park, C., Moon, D.Y., 2005. Characteristics of basalt fiber as a strengthening material for concrete structures. Compos. B Eng. 36, 504–512.
Soares, L.W.O., Braga, R.M., Freitas, J.C.O., Ventura, R.A., Pereira, D.S.S., Melo, D.M.A., 2015. The effect of rice husk ash as pozzolan in addition to cement portland Class G for oil well cementing. J. Petrol. Sci. Eng. 131, 80–85.
Souza, W.R.M., Bouaanani, N., Martinelli, A.E., Bezerra, U.T., 2018. Numerical simulation of the thermomechanical behavior of cement sheath in wells subjected to steam injection. J. Petrol. Sci. Eng. 167, 664–673.
Taylor, H.F.W., 1990. Cement Chemistry, first ed. Thomas Telford, London.
Vejmelková, E., Koňáková, D., Scheinherrová, L., Doleželová, M., Keppert, M., Černý, R., 2018. High temperature durability of fiber reinforced high alumina cement composites. Constr. Build. Mater. 162, 881–891.
Yanagisawa, K., Hu, X., Onda, A., Kajiyoshi, K., 2006. Hydration of β -dicalcium silicate at high temperatures under hydrothermal conditions. Cement Concr. Res. 36, 810–816.
Yang, T., Han, E., Wang, X., Wu, D., 2017. Surface decoration of polyimide fiber with carbon nanotubes and its application for mechanical enhancement of phosphoric acid-based geopolymers. Appl. Surf. Sci. 416, 200–212.